Design of the multi-cylinder Stirling engine arrangement with self-start capability and reduced vibrations

Design of the multi-cylinder Stirling engine arrangement with self-start capability and reduced vibrations

Jafar M. Daoud, Daniel Friedrich*

School of Engineering, Institute for Energy Systems, University of Edinburgh, EH9 3DW (Scotland)

**Corresponding author Email: d.friedrich@ed.ac.uk*

Abstract: *The Franchot engine is a double acting Stirling engine that has a freely controllable phase angle and no shuttle and axial conduction losses but is inferior to the Siemens and free piston Stirling engines in terms of its ability to self-start. In addition, the Franchot engine is not widely used with the reliable slider crank mechanism due to vibrations. Here, the multi-cylinder Franchot engine is thermodynamically and mechanically studied with the simple slider crank mechanism with the aim of improving the self-start capability and to reduce the vibrations. Both instantaneous power and engine arrangements are used to judge the mechanical performance for different engine parameters and configurations. The optimal phase shifts and phase angles are derived and it is shown that both are governed by the number of cylinders. The theoretical analysis shows that by increasing the number of cylinders, different engine vibrations are reduced and the engine becomes self-starting. Hence, the Franchot engine can be superior to the Siemens engine, particularly due to the ability to remove the rocking couples for engines with more than two phases. Thus, the engine operation is stabilised and the simple slider crank mechanism can be used with the multi-cylinder Franchot engine.*

Keywords: *Franchot engine; Stirling engine, double acting; multi-cylinder; phase angle; mechanical vibrations;*

1 Introduction

The Franchot engine which is a double acting Stirling engine was invented in the 19th century by Charles Louis Franchot [1]. In contrast to the double acting Siemens configuration, only two pistons are required, the phase angle can be freely controlled and each cylinder is either hot or cold which eliminates the shuttle and axial conduction losses [2]. It has been reported that, to complete the thermodynamic cycle in the Siemens configuration, at least three cylinders are needed to achieve the same phase angle between all hot and cold spaces [3][4][5]. This Siemens configuration produces consistent and continuous power through a cycle and hence can be self-starting. This self-starting capability is a significant advantage over the Franchot engine [6].

The number of cylinders affects the phase angle and phase shift of the Siemens engine. The phase angle is the thermodynamic angle between each expansion space and its corresponding compression space while the phase shift represents the angular distance between the expansion spaces. For each cylinder thermodynamically connected to an adjacent cylinder, the phase angle is given by $\theta = 180^{\circ} - \frac{360^{\circ}}{N}$ and the phase shift between reciprocating pistons is given by $\theta_S = \frac{360^{\circ}}{N}$. Here, N is the number of cylinders.

Chatterton and Pennacchi [7] showed that different thermodynamic connections can be made between multiple single acting engines with more than four cylinders which result in different phase angles. In addition, the net power increases with the number of engines, while the torque and rotational speed oscillations decrease. Similarly, multi-cylinder double acting engines can have more than one phase angle if each cylinder can be connected to any other cylinder and not only to adjacent cylinders. However, for any Stirling machine the preferred phase angle is within the range 90°-140° [8]. In this range of angles, the Siemens engine with a minimum of four cylinder is needed. At the phase shift of 120°, which can be obtained with the 3-cylinder engine, a non-recommended phase angle equal to 60° is obtained.

The thermodynamic cycle is complete for the Franchot engine with only one hot and one cold cylinder with an arbitrary phase angle, which is unconstrained by the configuration. It has not been reported that the single Franchot engine can be self-starting. However, it has been shown [9][10][11] that a dual Franchot engine could self-start if the two engines are phase shifted by 90^o, which is equivalent to the four cylinder Siemens configuration in terms of number of cylinders and phase shift. Arthur and Varela [9] patented a dual Franchot engine for a hybrid automotive. They suggested using dual Franchot engines working at the highest efficiency to drive a linear alternator to generate electricity. They suggested a synchronising crank to keep the volume and phase angles at the predefined value of 90^o. The SPP 4-106 engine [10] is a dual Franchot engine which uses the slider crank drive with a 90^o phase shift between the two Franchot engines but can use different phase angles. The 90^o phase shift gives the lowest torsional vibration and causes the engine to self-start. Fette [11] manufactured a liquid piston type dual Franchot engine. In which, all liquid pistons were phase shifted by 90^o using external solid pistons with a kinematic drive.

Double acting as well as single acting Stirling engines can use the simple slider crank drive [12][3] but at the cost of vibrations. The Franchot and dual Franchot engines have an uneven distribution of masses and cranks, which creates dynamic imbalances. These imbalances cause first order vibrations such as reciprocal vibration (i.e. those caused by the up and down piston motion) and rocking couples (i.e. those created due to the offset between pistons). Rocking couples are opposite force twins that cause force moment responsible for the vibration along the crankshaft. Reciprocal vibrations and rocking couples are found in single acting Stirling engines due to the phase angle while rocking couples are found in the Siemens configuration as a result of the absence of piston pairs. Thus, the Siemens engine was brought to practice with the swash plate and wobble yoke [6][13][14]. The wobble yoke has been commercialised at the maximum possible number of cylinders of 4 [7]. Walker [1] suggested using the wobble drive with the Franchot engine for railway applications. Due to the uneven distribution of pistons the Stiller drive is reported to be used with the dual Franchot engine with a phase shift of 90^o [15]. In addition, the Stirling engines vibrations can be reduced by methods of reducing the charge pressure or dynamic balancing which adds counterweights to the crankshaft [16][17]. Dynamic balancing can effectively remove vertical vibrations but creates horizontal vibrations hence there will be a need to reduce the reciprocating masses [18][19].

Alternatively, in internal combustion engines, vibrations due to the primary forces, which have the same frequency as the engine rotation can be removed by an inherent balance, in which many cylinders participate in generating opposite vibrations that cancel each other out [20]. For example, the reciprocal vibration caused by a moving piston can be eliminated by another piston moving exactly opposite to the first piston. For a three-piston engine, reciprocal vibrations are reduced if the pistons are apart by 120^o degree. However, rocking couples still exist due to the offset between pistons. For the 4-cylinder engine, two pistons in the middle move with each other while the outer pistons move with each other and opposite to the middle couple. Hence, reciprocal and rocking vibrations are reduced. Moreover, torsional vibration caused by power pulses on the crankshaft are reduced due to uniform distribution of power strokes. To the best of the authors' knowledge, inherent balance has not been applied to Stirling engines yet. The rocking couples can be removed by piston pairs moving together. While this could be achieved for the Franchot engine, it is not possible for the Siemens engine. Attribution is made to the Siemens engine because it is a multi-cylinder and double acting engine which is preferable over the Franchot engine for its ease of sealing, simpler kinematics and self-starting capability.

In their attempt to get rid of complex heat exchangers, Daoud and Friedrich [21] suggested a new heat exchanging mechanism for which, heat is added and rejected directly through the cylinder walls of the

Franchot engine. Their polytropic model considers heat addition and removal during the expansion and compression processes hence they are not isothermal or adiabatic but polytropic. Later, the same authors [22] proposed hot and cold isothermalisers for the Franchot engine to increase the power and efficiency and reduce the gas flow rate which helps in reducing the pumping losses. They modified the polytropic model to include the gas friction losses and enhanced heat transfer in the cylinders and found that the gas friction can be ignored up to the maximum power. However, increasing the number of cylinders can lead to an increase in the power similar to the isothermalisers which have some geometric limitations. Recently, Daoud and Friedrich [23] proposed a new free piston Franchot engine based on the balanced compounding technique using multiple cylinders. They used a dynamic model based on the polytropic model and showed that, the free piston Franchot engine is possible and can use long cylinders with small bores. However, there is a lack of experimental and theoretical research on the self-starting and vibration reduction of Stirling engines and especially kinematic Stirling engines [23][24].

In this theoretical study, we derive guidelines for the design multi-cylinder Franchot engines with improved mechanical performance of the kinematic engine. The study uses a validated polytropic model and phasor diagrams to evaluate the power pulses and mechanical piston arrangements of multi-cylinder Franchot engines. The results enable the design of multi-cylinder engines with the simple slider crank drive, which have the capability to self-start and have reduced torsional and primary vibrations on the crankshaft.

2 Methodology

A kinematic Stirling engine can start up if the total work over a complete cycle is positive [24]. A single-acting Stirling engine with kinematic drive generates negative power durations due to the compression stroke. To guarantee the power hence motion continuity, a flywheel is commonly used to overcome the negative power durations and reduce generated harmonics by using some of its stored kinetic energy [25]. At engine start-up, an external mechanical force is required to bring the engine above the stalling speed. If the force is not adequate the engine will slow down until it completely stops. The stored energy in a solid cylinder flywheel is given by:

$$k_e = 0.5\, J\, \omega^2 \qquad (1)$$

where J and ω are the flywheel moment of inertia and angular velocity, respectively.

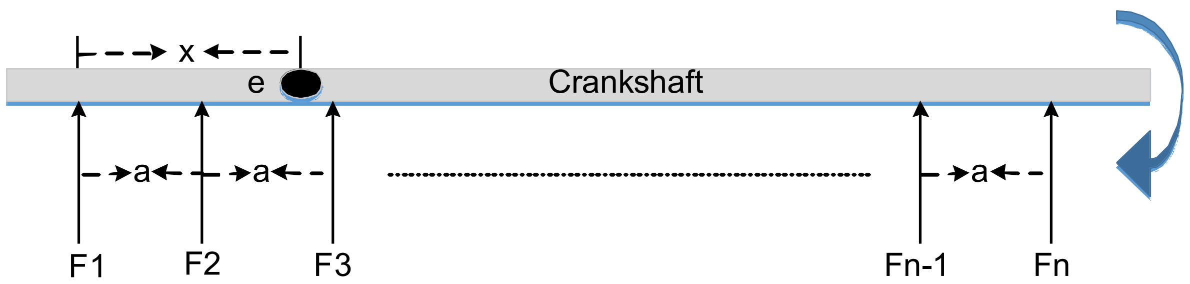

Figure 1: Free body diagram of a rotating crankshaft showing piston forces.

Here, a strict assumption is made that not only the average power should be positive but also the instantaneous power generated by the engine should always be positive. This implies that the average power is positive and the engine starts up at low speeds at which the kinematic energy of the flywheel is negligible, thus leads to self-starting. The instantaneous power will be used to check the power continuity and power pulses that cause torsional vibrations on the crankshaft of a slider crank mechanism without using a flywheel. The reciprocal and rocking vibrations will be investigated according to the inherent balancing method based on the phasor diagram and cylinder arrangement. A rotating shaft is dynamically balanced if it is statically balanced and the resulting turning moment is zero which is obtained if there is a uniform distribution of moving masses on the crankshaft. To remove the rocking couples in the inline topology, the algebraic sum of the couples at any point in the plane of cylinders should be zero. If the offset between force signals along the crankshaft is the same (see Figure 1), the force moment at any point on the crankshaft is written as

$$\sum M_e = 0 \tag{2}$$

hence,

$$\overrightarrow{F_1}x + \overrightarrow{F_2}(x-a) + \overrightarrow{F_3}(x-2a) \ldots + \overrightarrow{F_n}(x-(n-1)a) = 0 \tag{3}$$

When the pistons are pairwise coupled (i.e. $\overrightarrow{F_1} = \overrightarrow{F_n}, \overrightarrow{F_2} = \overrightarrow{F_{n-1}}, \ldots.$), Equation 3 becomes

$$\overrightarrow{F_1}(2x-(n-1)a) + \overrightarrow{F_2}(2x-(n-1)a) + \cdots = 0 \tag{4}$$

hence,

$$(2x-(n-1)a)\sum_{i=1}^{n/2}\overrightarrow{F_i} = 0 \tag{5}$$

Thus, to eliminate the vibrations due to rocking couples, piston couples should exist, the offset between pistons needs to be the same and the vector summation of the primary forces must be zero which implies that the moving masses have to be uniformly distributed around the crank shaft.

The ideal instantaneous power is given by

$$P_{ins} = (p - p`)(\dot{v}_e + \dot{v}_c) \tag{6}$$

where p, P, v_e and v_c represent the instantaneous pressure, instantaneous power, expansion volume and compression volume and the notation (`) represents the variables of the opposite piston side.

The compression volume of the Franchot engine is calculated from

$$v_c = 0.5\, V_{sw}(1 + \cos(\omega t + \theta_s)) + V_{dead} \tag{7}$$

correspondingly, the expansion volume is calculated from

$$v_e = 0.5\, V_{sw}(1 + \cos(\omega t + \theta + \theta_s)) + V_{dead} \tag{8}$$

where θ, θ_s, V_{sw} and V_{dead} are the phase angle, phase shift between a Franchot engine and an arbitrary zero position, swept volume and dead volume, respectively. The swept and dead volume are calculated from

$$V_{sw} = \frac{\pi D^2}{4}L \tag{9}$$

$$V_{dead} = \frac{\pi D^2}{4}r \tag{10}$$

where, $D, L\ and\ r$ are the piston diameter, stroke length and clearance volume, respectively. As the swept volumes are sinusoidal, Equation 6 can be written as

$$= p(\dot{v}_e + \dot{v}_c) + p`\left(\grave{\dot{v}}_e + \grave{\dot{v}}_c\right) = P + P` \tag{11}$$

The total power transferred to the crankshaft of a Franchot engine (see Figure 5) is the summation of power generated by Stirling engines on both sides of the power piston. Assuming the engine is symmetrical for both sides, the power of the opposite Stirling engine is the power of a Stirling engine shifted by 180^o. Hence, the instantaneous power of the Franchot engine can be calculated by considering only one side of the Franchot engine as

$$P_{ins} = p(\dot{v}_e + \dot{v}_c) + \ p(\dot{v}_e + \dot{v}_c)\angle 180^o \tag{12}$$

where the second part of the equation is the instantaneous power of a Stirling engine shifted by 180^o (indicated by $\angle 180^o$ according to notation for multiphase systems).

Similarly, the instantaneous power of any Franchot engine in a multi-engine configuration can be obtained based on the phasor diagram for different phase shifts without rebuilding distinct equations for each engine by

$$P_{ins} = [p(\dot{v}_e + \dot{v}_c) + \ p(\dot{v}_e + \dot{v}_c)\angle 180^o]\angle\theta_s \tag{13}$$

for

$$0^o \leq \theta_s \leq 360^o \tag{14}$$

By considering only one alpha engine, the number of variables, complexity of the model and the simulation time are reduced. The pressure variation on one side of the direct cylinder heated and cooled Franchot engine is calculated from [21]

$$\dot{p} = \frac{-p\left(\frac{\dot{v}_e}{T_{re}} + \frac{\dot{v}_c}{T_{cr}}\right) + \frac{R}{c_p}\left(\frac{\dot{Q}_e}{T_{re}} + \frac{\dot{Q}_c}{T_{cr}}\right)}{\frac{v_e}{\gamma T_{re}} + \frac{V_r}{T_r} + \frac{v_c}{\gamma T_{cr}}} \tag{15}$$

where $v\,, T, and\ \dot{Q}$ denote the volume, temperature and heat flow rate in the working spaces, respectively, and subscripts $e, r\ and\ c$ indicate the expansion, regeneration and compression space, respectively.

Regenerator end temperatures are calculated from [21]

$$T_{rh} = \frac{-\oint i\dot{m}_e T_e}{\oint (1-i)\dot{m}_e} \tag{16}$$

$$T_{rk} = \frac{-\oint j\dot{m}_c T_c}{\oint (1-j)\dot{m}_c} \tag{17}$$

where the parameters i and j are given by

$$i = \begin{cases} 1, & \dot{m}_e < 0 \\ 0, & \dot{m}_e \geq 0 \end{cases} \tag{18}$$

$$j = \begin{cases} 1, & \dot{m}_c < 0 \\ 0, & \dot{m}_c \geq 0 \end{cases} \qquad 19$$

Hence, the average regenerator temperature is

$$T_r = \frac{T_{rh} - T_{rk}}{\ln \frac{T_{rh}}{T_{rk}}} \qquad 20$$

External irreversibility is considered through the heat addition and removal which are calculated from Newton's law of cooling [26]

$$\dot{Q} = hA\Delta T \qquad 21$$

where h is the convective heat transfer coefficient, which holds for Reynolds' numbers between 1000 and 100,000 and is calculated as [27]

$$\begin{aligned} h_e &= 0.042 {D_h}^{-0.42} v^{0.58} p^{0.58} T^{-0.19} \\ h_c &= 0.0236 {D_h}^{-0.47} v^{0.53} p^{0.53} T^{-0.11} \end{aligned} \qquad 22$$

where $\Delta T, D_h, h_e \; and \; h_c$ are the temperature difference between the working gas and cylinder wall, hydraulic diameter, convective heat transfer during the expansion and compression, respectively.

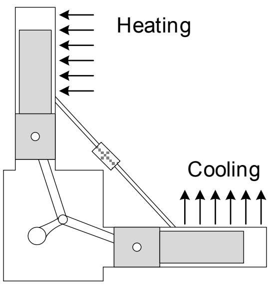

Figure 2: Schematic of the Karabulut alpha type engine with annular heat exchangers.

For validation, the polytropic model is applied to the alpha type engine with annular heat exchanger made by Karabulut [28]. In the Karabulut engine shown in Figure 2 , the heat exchanging area and volume are constant for the annulus and dynamic for the swept space. These conditions are replicated in the model for validation purpose. The technical specification of the engine is shown in *Table 1*.

Table 1: Technical specifications and operating conditions of Karabulut engine [28].

Name	***Value and unit***
Stroke length	*6 cm*
Bore diameter	*5.24 cm*
Piston dome diameter	*4.74 cm*
Hot annulus length	*13.5 cm*
Cold annulus length	*11 cm*
Connecting pipe length	*30 cm*
Connecting pipe diameter	*0.5 cm*
Regenerator matrix	*Woven wire*
Wire diameter	*100 micron*

Regenerator porosity	*0.7*
Regenerator volume	*12 cm^3*
Out-of-Phase angle	*90^o*
Hot, cold temperatures	*1100^{o}C ,20^{o}C*
Working gas	*Air*
Average gas pressure	*1 bar, 2 bar*

To increase the accuracy of the model the reheat and pressure losses of the regenerator are considered. The effect of having imperfect regeneration is considered by modifying the regenerator gas stream temperatures as [29][30]

$$T_{rho} = T_{rk} + \varepsilon(T_{rh} - T_{rk}) \quad 23$$
$$T_{rko} = T_{rh} - \varepsilon(T_{rh} - T_{rk}) \quad 24$$

where, $T_{rho}, T_{rko}\ and\ \varepsilon$ are the hot outlet gas temperature, cold outlet gas temperature and regenerator effectiveness, respectively.

The effectiveness is calculated according to Tanaka [31] by

$$\varepsilon = \frac{Ntu}{Ntu + 2} \quad 25$$

where Ntu is the number of transfer units and calculated from

$$Ntu = \frac{4\overline{Nu}L_r}{P_r\overline{R_e}d_h} \quad 26$$

where $\overline{Nu}, P_r, \overline{R_e}\ and\ d_h$ are the average Nusselt number, Prandtl number, average Reynolds number and regenerator hydraulic diameter, respectively.

The Nusselt number is correlated according to Tanaka as follows

$$\overline{Nu} = 0.33\overline{R_e}^{0.67} \quad 27$$

The pressure loss due to the gas friction with the regenerator material is calculated from

$$\Delta p_{loss} = -\frac{0.5 f_h \rho L_r U^2{}_{max}}{d_h} \quad 28$$

where Δp_{loss} is the pressure loss and f_h is the friction factor calculated according to Tanaka from

$$f_h = 1.6 + \frac{175}{Re_{max}} \quad 29$$

The pressure loss due to the connecting pipe is calculated as

$$\Delta p_{loss} = -\frac{2 f_{Re} \mu L_r U_{av}}{d_h} \quad 30$$

where f_{Re} is calculated by [32]

$$f_{Re} = \begin{cases} 16 & Re < 2000 \\ 7.343 * 10^{-4} Re^{1.3142} & 2000 < Re < 4000 \\ 0.0791 Re^{0.75} & Re > 4000 \end{cases} \quad 31$$

The model is implemented in Matlab/Simulink and the ordinary differential equations 15 and 21 are solved with the Runge-Kutta method with a time step of 10^{-4}s. A number of simulations at different frequencies was performed with a time step of 10^{-5}s. These showed only negligible differences so that the time step of 10^{-4}s was used for all simulations.

The mathematical model is applied to the Karabulut engine at a range of speeds and two pressures. The comparison between the polytropic model and experimental study is shown in Figure 3. The polytropic model has reasonably good agreement with the experimental results especially in predicting the trend of engine performance and location of the power peak values. The maximum relative error was calculated as 22% and 30% for the 1 and 2 bar data sets, respectively. Those errors can be attributed to the roughness of the experimental data, the lack of data about gas leakage and mechanical friction. In addition, these errors are located far away from the power peak operation. Thus, this validation gives confidence that the polytropic model can accurately predict the operating conditions and power peak of the Franchot engine.

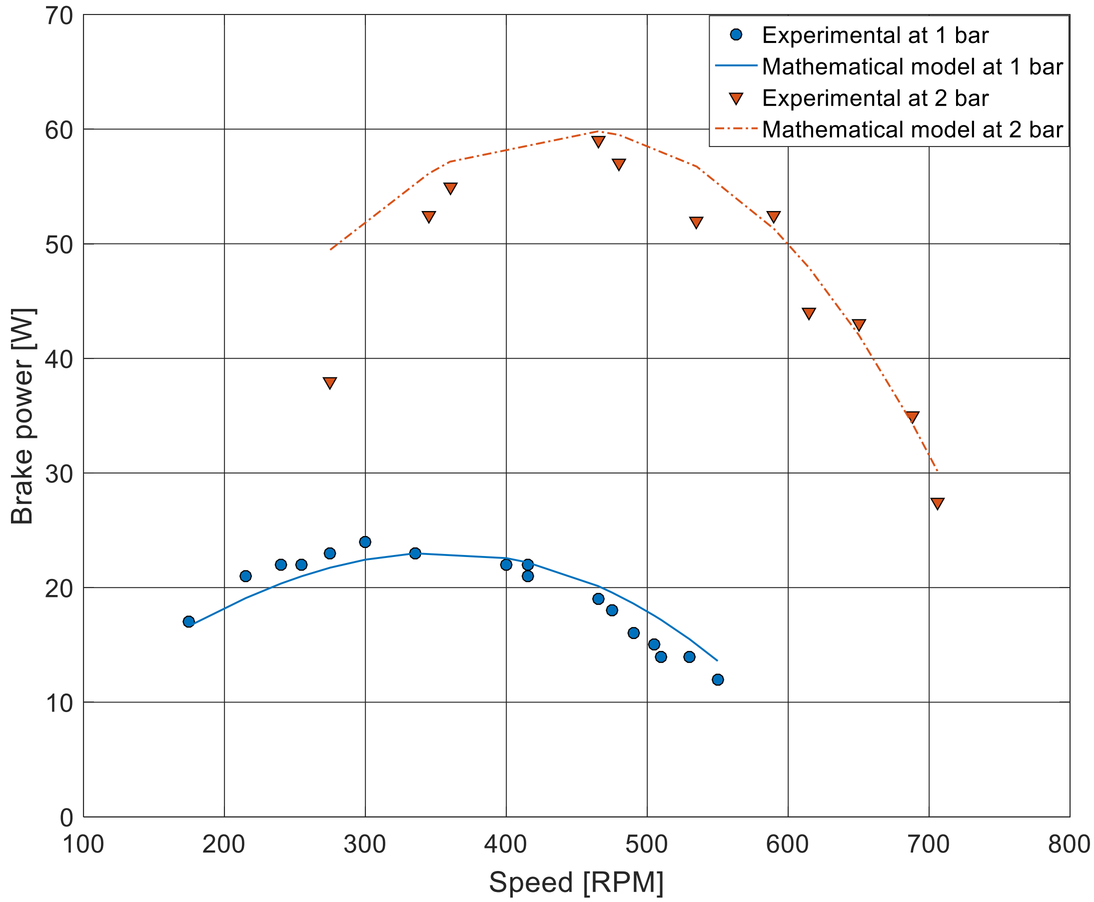

Figure 3: Comparison between the 3 control volume polytropic model with regenerator losses and experimental data of Karabulut alpha type engine [28].

3 Results and discussion

The reported instantaneous powers were generated once the simulation reached the quasi-steady state condition. All results use the reference engine parameters listed in Table 2 unless otherwise stated. The PV diagram of the studied engine is shown in Figure 4.

Table 2: Parameters of the reference engine

Name	symbol	value/unit
Stroke length	L_e, L_c	50 cm
Bore diameter	D_e, D_c	0.75 cm
Gas density	ρ	1.225 kg/m^3
Clearance length	re, rc	0.1 mm
Reg. volume	V_r	0 cm^3
Phase angle	θ	120°
Temperatures	T_h, T_k	450 K,300 K

Rotation speed	n	500 RPM,
Working gas	Air	
Gas constant	R	287 J/kg.K

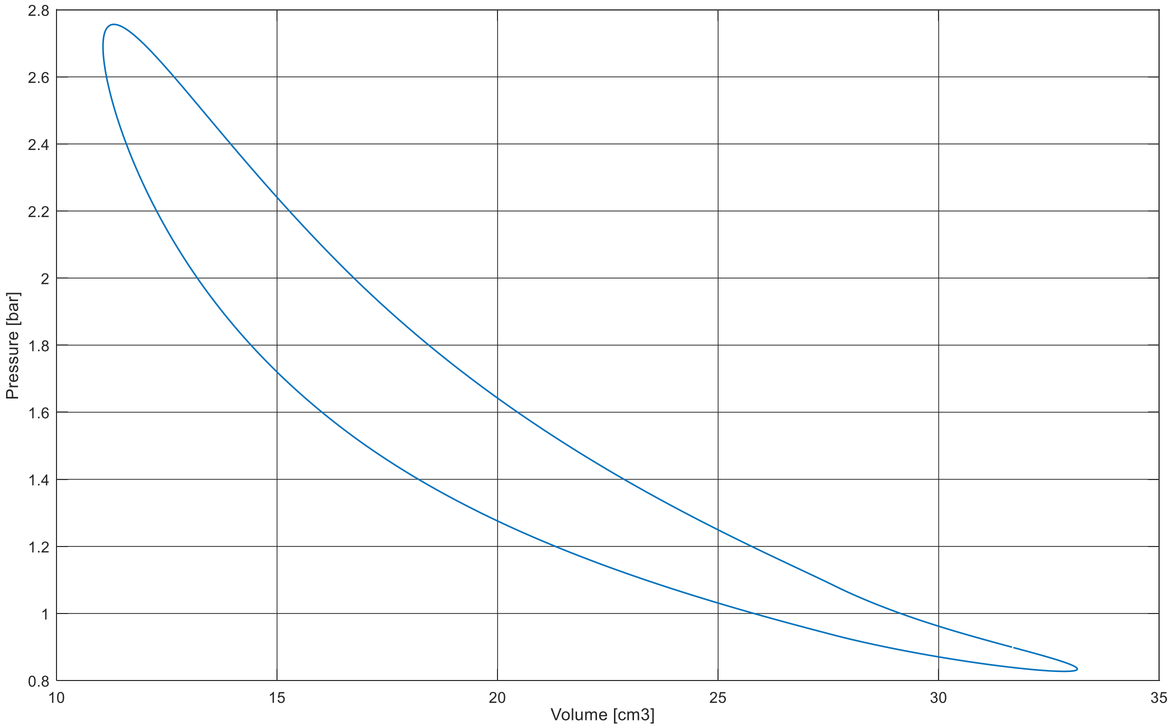

Figure 4:PV diagram of the reference engine.

3.1 Single phase (1-ph) Franchot engine

This is the simplest engine configuration that has only a pair of hot and cold cylinders connected to each other by two regenerators. The expansion volume v_e is always leading the compression volume v_c by an arbitrary phase angle. The phasor diagram of the 1-ph Franchot engine in Figure 5 shows that forces and masses are not uniformly distributed around the crankshaft, which causes vibrations. The phase angle controller is used to define the optimal phase angle between the expansion and compression spaces which is one of the advantages of the Franchot engine over the Siemens engine. While the masses will be uniformly distributed at a phase angle of 180^{o}, the total engine volume (expansion, compression and dead volume) for each Stirling engine is constant and the engine will stall.

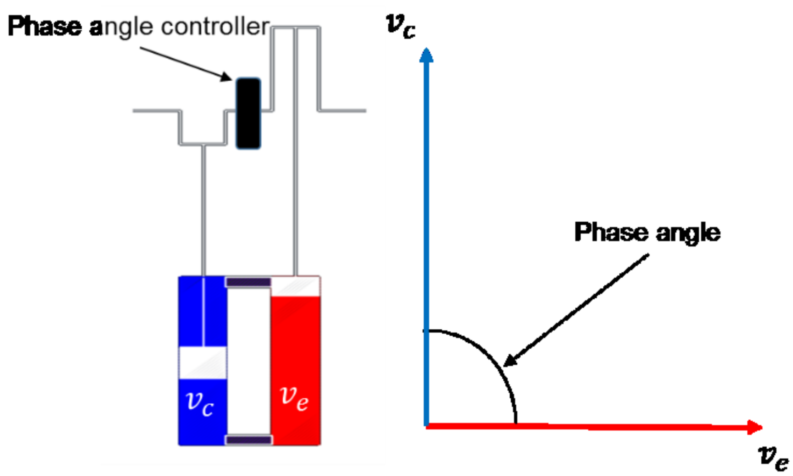

Figure 5: 1-ph kinematic Franchot engine and its phasor diagram.

The start-up capability of the Franchot engine is investigated with respect to the temperature, phase angle and dead volume (the clearance volume in the engine cylinders). Figure 6 shows that negative power is reduced but not eliminated for the studied cases. Increasing the temperature increases the power variation and reduces the negative part of the power by shifting the power curve up due to the increasing pressure in the expansion stroke. Increasing the dead volume to 100% of the swept volume reduces the power variations which is due to the reducing pressure variations. Increasing the phase angle leads to a reduction in the negative part of the power signal without eliminating it completely. The reduction is due to the decreasing pressure variation and time shift between negative and positive power peaks. The latter works as a filter for the power signal while reducing the pressure variation reduces the power signal amplitude so that it oscillates around zero as the volumes on both sides of the working pistons approach equality. Thus, an increase in the dead volume increases the impact of the negative power durations. It can be concluded that the $1 - ph$ Franchot engine does not have the capability to self-start or run without a flywheel by increasing the input temperature, dead volume or phase angle.

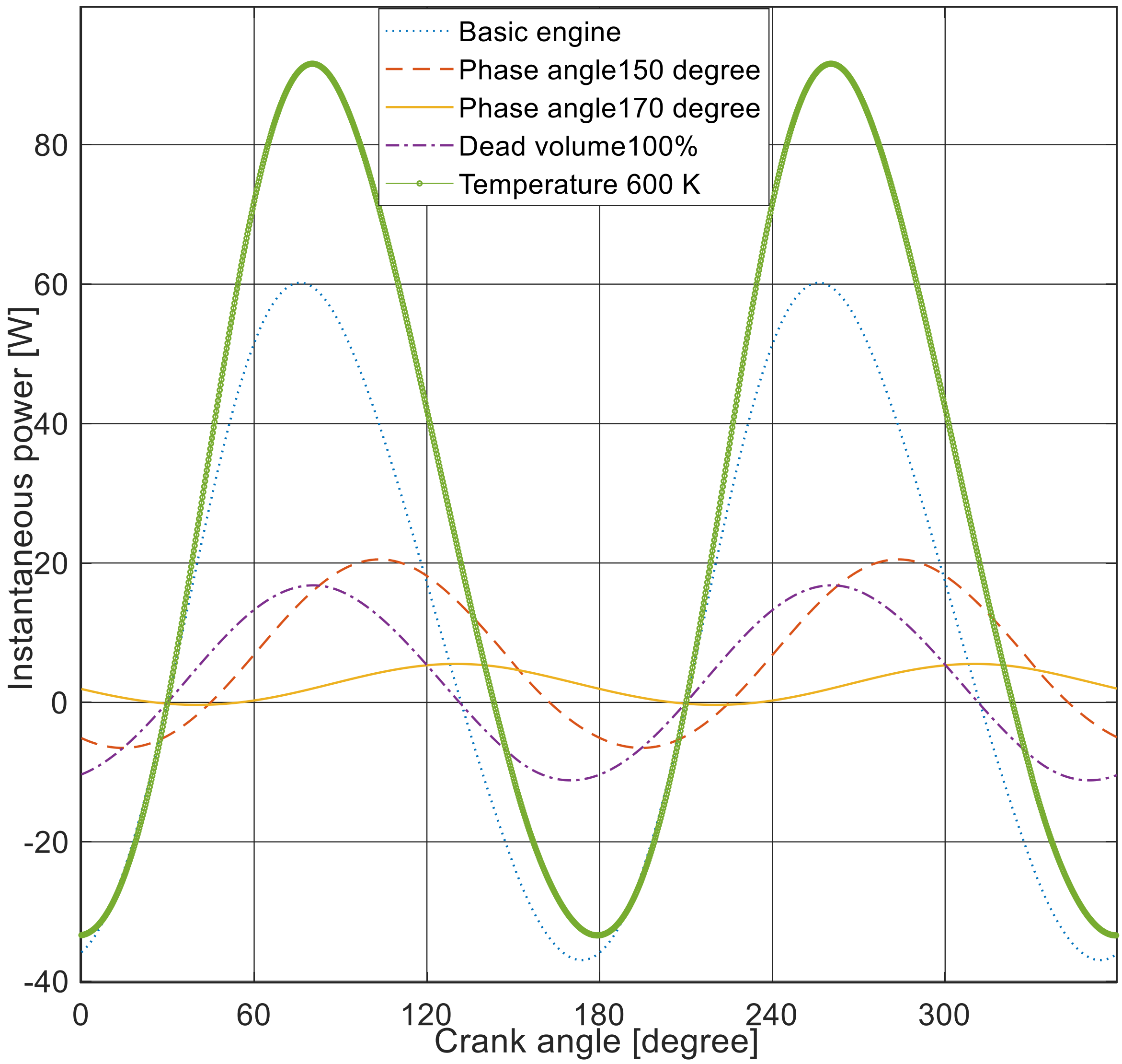

Figure 6: Power Response for increasing the phase angle, dead volume and temperature of the reference engine.

Figure 7 shows that the instantaneous powers of the opposite Stirling engines do not negate each other because otherwise, the generated power would be zero. The frequency of the combined power signal P_{ins} of the double acting Franchot engine is twice the frequency of an alpha engine because the individual instantaneous powers are not sinusoidal and the shifted power peaks do not match with the original peaks. Høeg et al. [10] also showed that the torque signal frequency is twice the engine rotation frequency. Therefore, the Franchot engine has two negative power regions in one rotation, which are smaller in magnitude than the negative power of a duplicated alpha engine. In a duplicated alpha engine, the negative powers are added together whilst in the Franchot engine, negative and positive powers are added which reduces the power variations hence torsional vibrations.

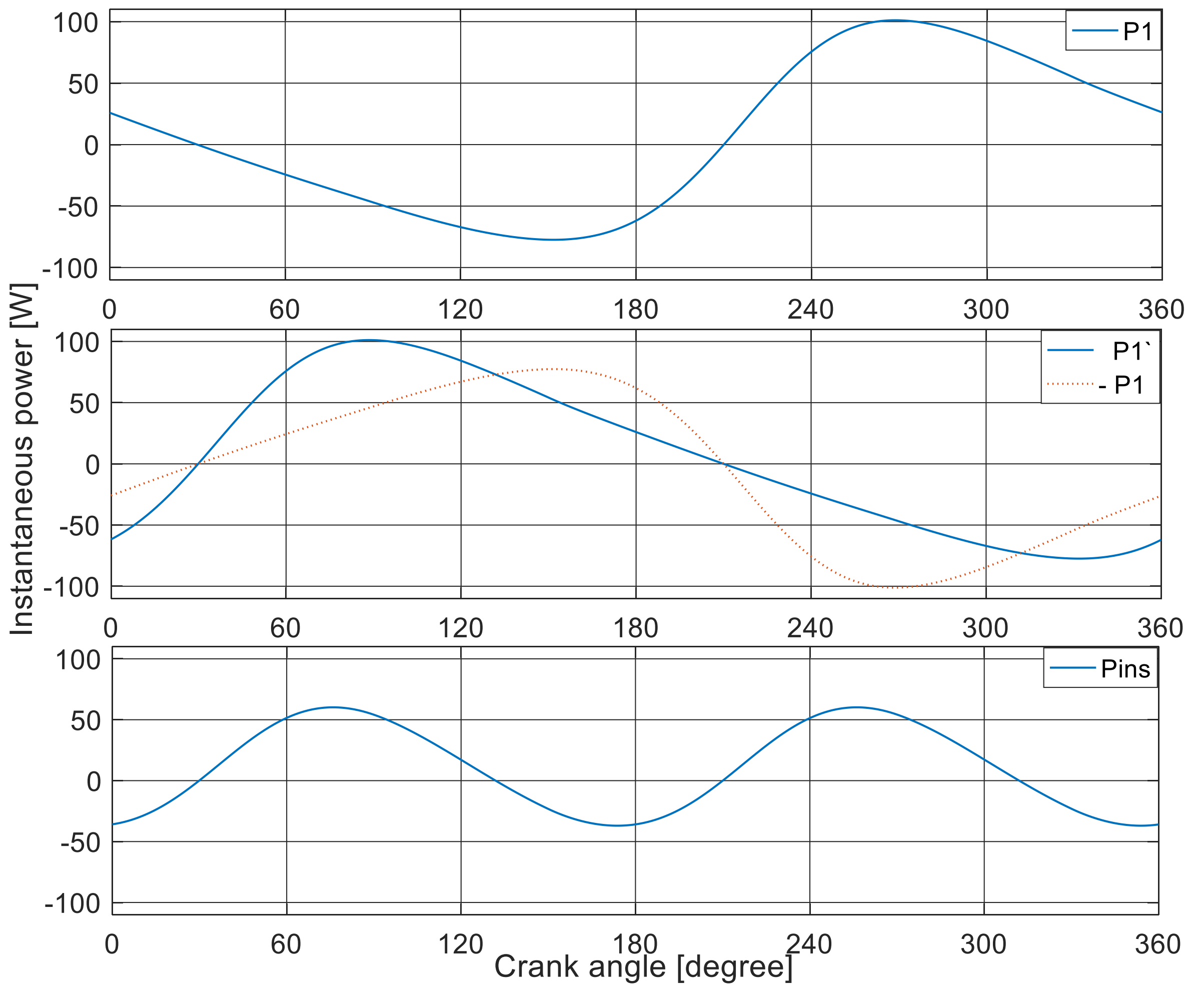

Figure 7: Instantaneous power response at the steady state of the reference engine showing the power of one side, the difference between the shifted and negated power and the total instantaneous power of the reference Franchot engine.

3.2 Dual phase (2-ph) Franchot engine

The dual Franchot engine is comprised of two Franchot engines connected to a slider crank drive in inline topology. The dual Franchot engine can be mechanically coupled to the crankshaft in inline configurations where there is an arbitrary phase shift between any of the two hot or cold cylinders. Figure 8 shows a dual Franchot engine for which the phase angle can be controlled with a single device and which uses a common heater and a common cooler. The phasor diagram in Figure 8 shows that the dual Franchot engine is prone to vibrations due to the uneven distribution of cranks and masses unless the phase shift is set to 180°. However, at a phase shift of 180° or multiples thereof, the thermodynamic performance of the dual engine is similar to the 1-ph engine (see Figure 9).

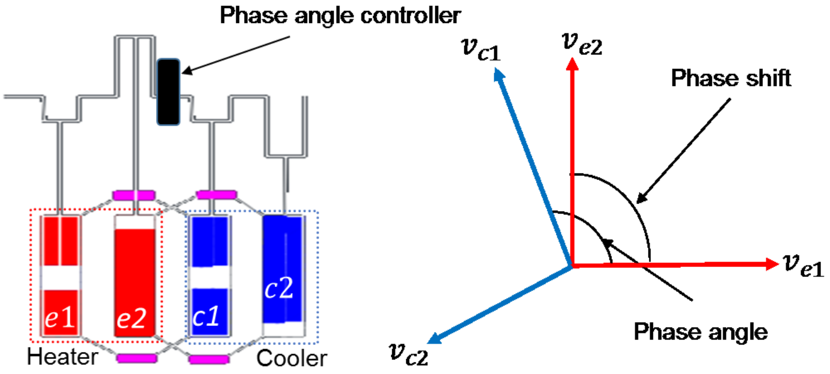

Figure 8: Dual kinematic Franchot engine and its phasor diagram.

Figure 9 shows that the lowest power variation occurs at the 90° phase shift. The same angle was confirmed experimentally for causing the minimum torque variations by Høeg et al. [10]. Thus, the dependency on a flywheel is reduced and the self-starting properties are better than for the 1-ph Franchot engine, although small negative power durations still exist at the studied speed.

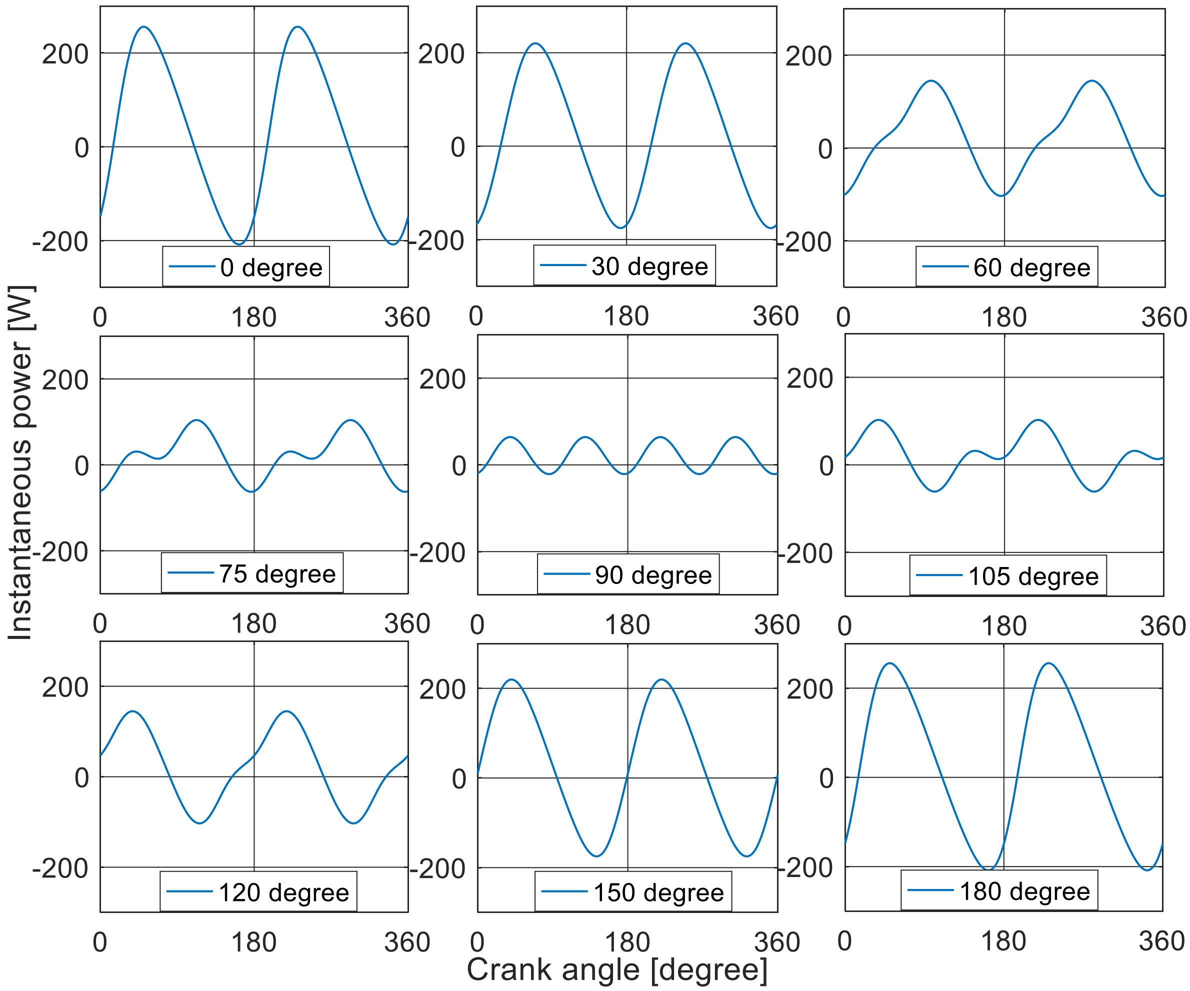

Figure 9: Effect of the phase shift on the power variation of a 2-ph Franchot engine at 90° phase angle.

The largest reduction in power variation occurs when the instantaneous powers of two Franchot engines are added with a 180° shift in power signal. In this case, each negative power duration is matched with a positive power duration in the opposite engine. The 180° shift in power signal is achieved for a 90° phase shift because the power wave frequency is twice the engine rotation frequency (see Figure 7). At a 90° phase shift, the power frequency of the 2-ph engine is four times the rotation frequency. Similarly, the phase shifts of 0° and 180° produce 0° and 360° phase shifts in the power wave, respectively and thus no shift in the power signal. Therefore, two or more engines with 0° or 180° phase shift are just a 1-ph Franchot engine with multiple cylinders.

Figure 10 shows the capability of the 2-ph Franchot engine with a phase shift of 90° to self-start. This finding is in line with former studies [9][10][11]. The low speed represents the response of the system just after starting. At low speed, the compression process is almost isothermal due to the long cycle time, which reduces the negative power needed for compression. Thus, the engine will continue running beyond 30 RPM with a flywheel as the negative power duration vanishes at low speeds. Increasing the temperature to 600K leads to an increase in power variations as well as in the average power. Hence, the positive shift in the average power removed the negative power durations. However, most important is the phase angle which acts as a filter of the power signal by reducing the pressure variations and hence the power variations. The instantaneous power for the increased phase angle of 120° leads to a uniform positive power, which has no negative durations. Hence, the 2-ph Franchot engine can be self-starting as the negative power durations vanish for increased temperature difference, decreased speed or increased phase angle. However, the engine is still generating power pulses, which makes the engine dependent on a flywheel to run smoothly, and the cranks are still unevenly distributed.

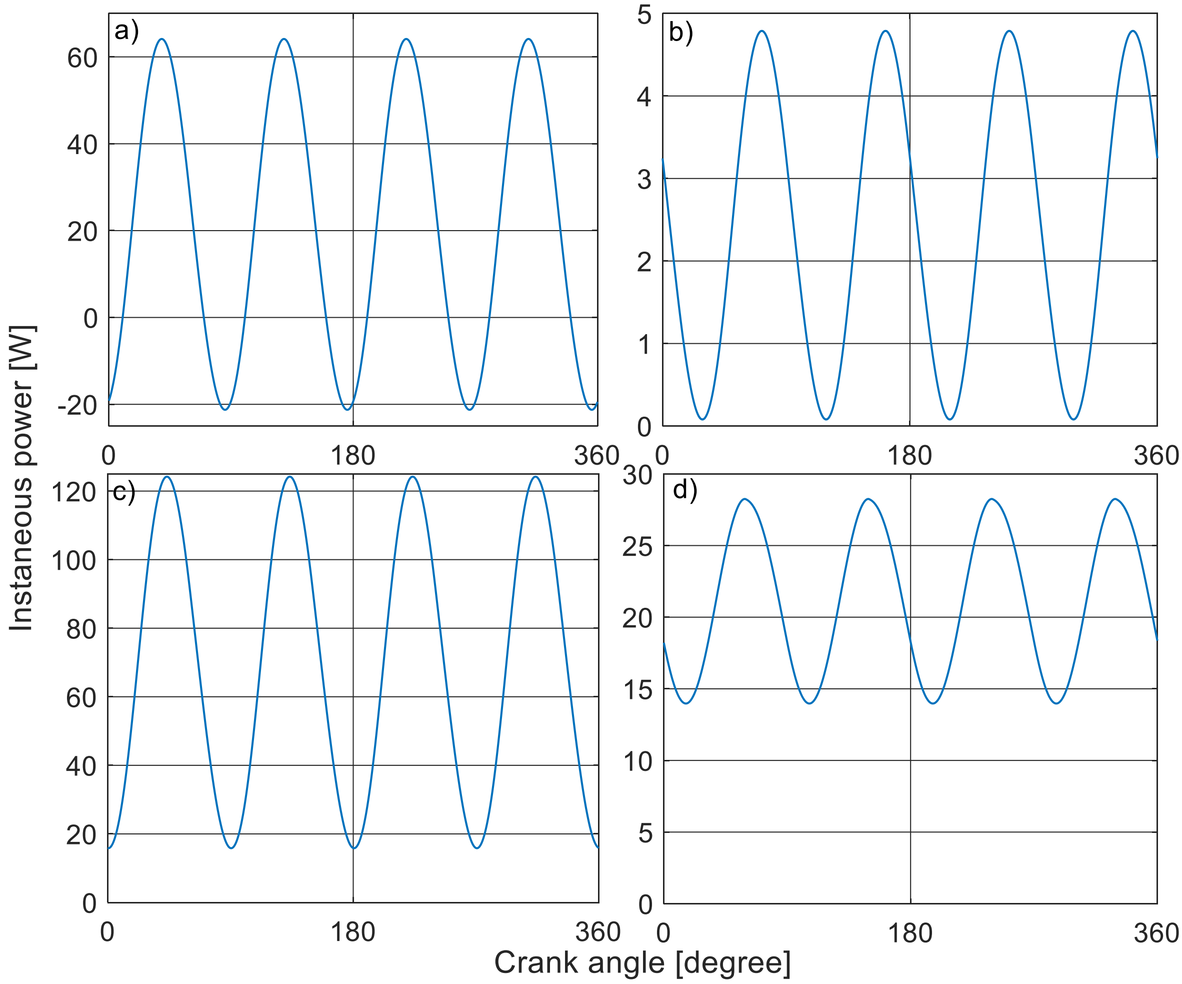

Figure 10: Instantaneous power of dual Franchot engine at phase shift of 90° and a) phase angle of 90° b) phase angle of 90° and n = 30 rpm c) phase angle of 90° and Th = 600K d) reference engine at phase angle of 120°.

3.3 Three phase (3-ph) Franchot engine

The 3-ph Franchot engine shown in Figure 11 is arranged in an inline topology in the slider crank mechanism so that there are a common heater, a common cooler and one device to control the phase angle. As each Franchot engine has two regenerators, this arrangement has a twin of longer regenerator connections between cylinder e1 and c1 in comparison to the other connections. The phasor diagram (Figure 11) shows a uniform distribution of the masses and forces on the crankshaft which removes the vibrations caused by the unbalanced forces and masses. The phasor diagram shows the reciprocal vibrations vanish even if the phase angle is controlled as the vector summation of the forces is zero for arbitrary phase angles. In addition, it is also possible to remove the rocking couples if the phase angle equals the phase shift. At this phase angle, the engine has piston twins (e1-c3, e2-c1 and e3-c2) that move with each other. Therefore, to reduce the primary vibrations, both the phase shift and phase angle have to be fixed to 120^{o}. By swapping the location of cold cylinders c1 and c2 the engine would have equal regenerator lengths but the rocking couples will not be inherently removed.

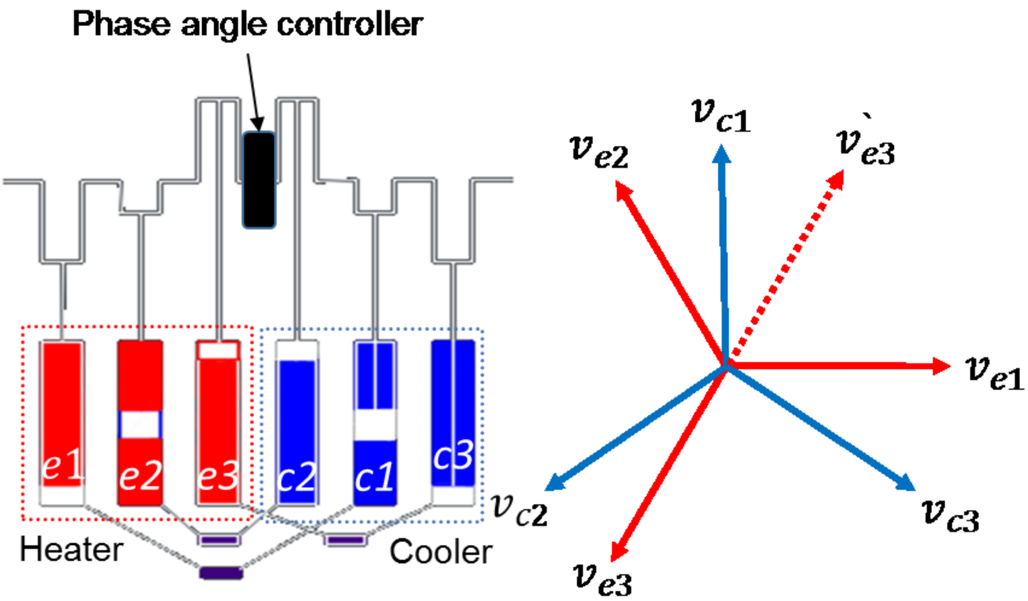

Figure 11: 3-ph kinematic Franchot engine and its phasor diagram.

Figure 12 shows that there are two phase shifts (60^{o} and 120^{o}) at which the system has the minimum power variation. At these angles, the power frequency is three times the power pulse frequency or six times the rotational frequency of a 1-ph Franchot engine. The minimum instantaneous power is shifted to a positive value and the power variation on the crankshaft is reduced.

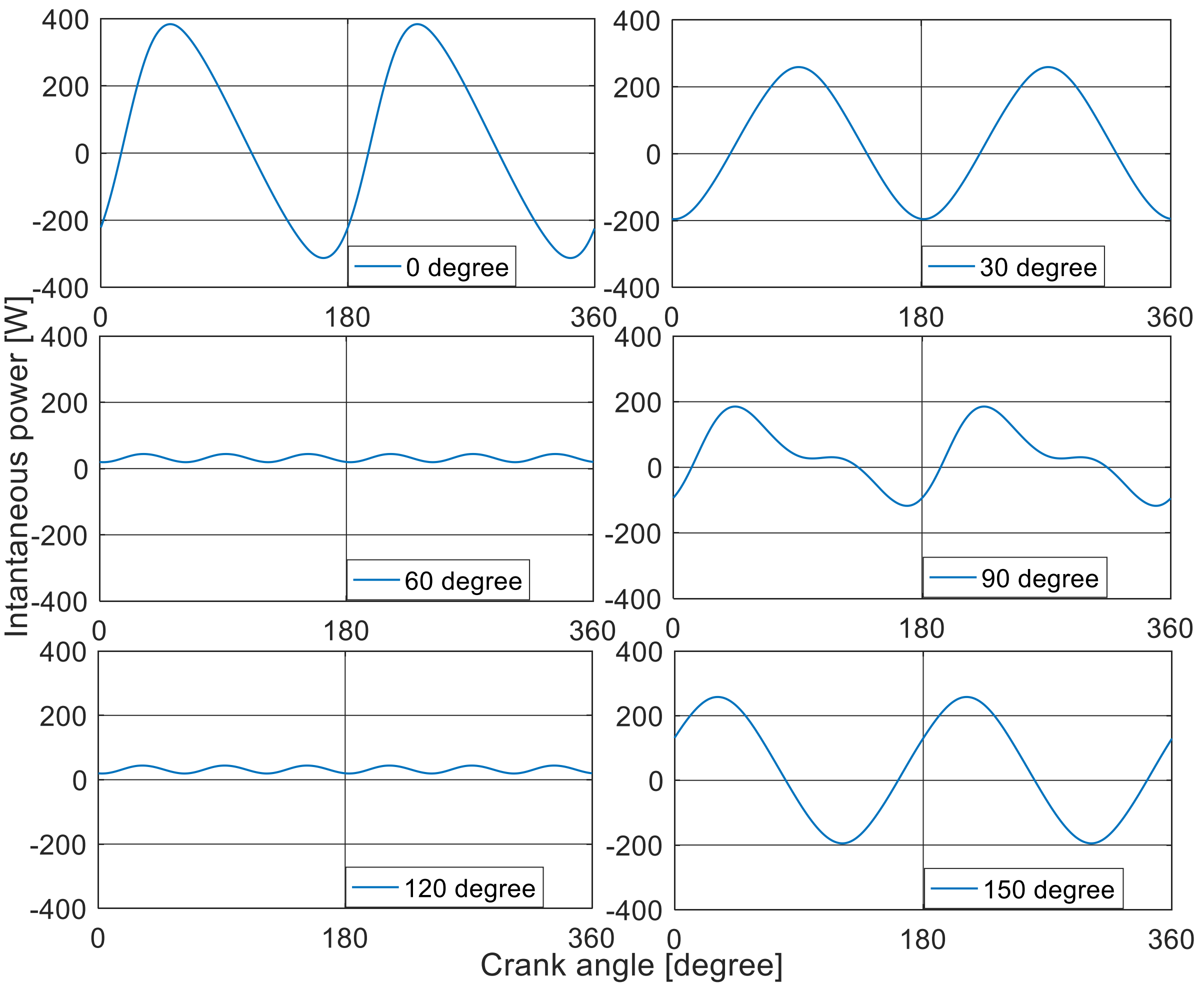

Figure 12: Effect of the phase shift on the instantaneous power of the 3-ph Franchot engine at 90º phase angle.

Figure 13 shows the power response of the 3-ph Franchot engine is similar at phase shifts of 60º and 120º for different phase angles. The reason for this is that the Franchot engine has two Stirling engines mounted mechanically opposite to each other and thus, the 60º corresponds to 120º for the opposite engine as it is shifted by 180º (see Figure 11). In addition, larger phase angles lead to smaller power variations hence smoother power signals. These power variations are much smaller than in the 2-ph Franchot engine (see Figure 9). Therefore, the need for a flywheel is much smaller for the 3-ph Franchot engine than for the 2-ph engine.

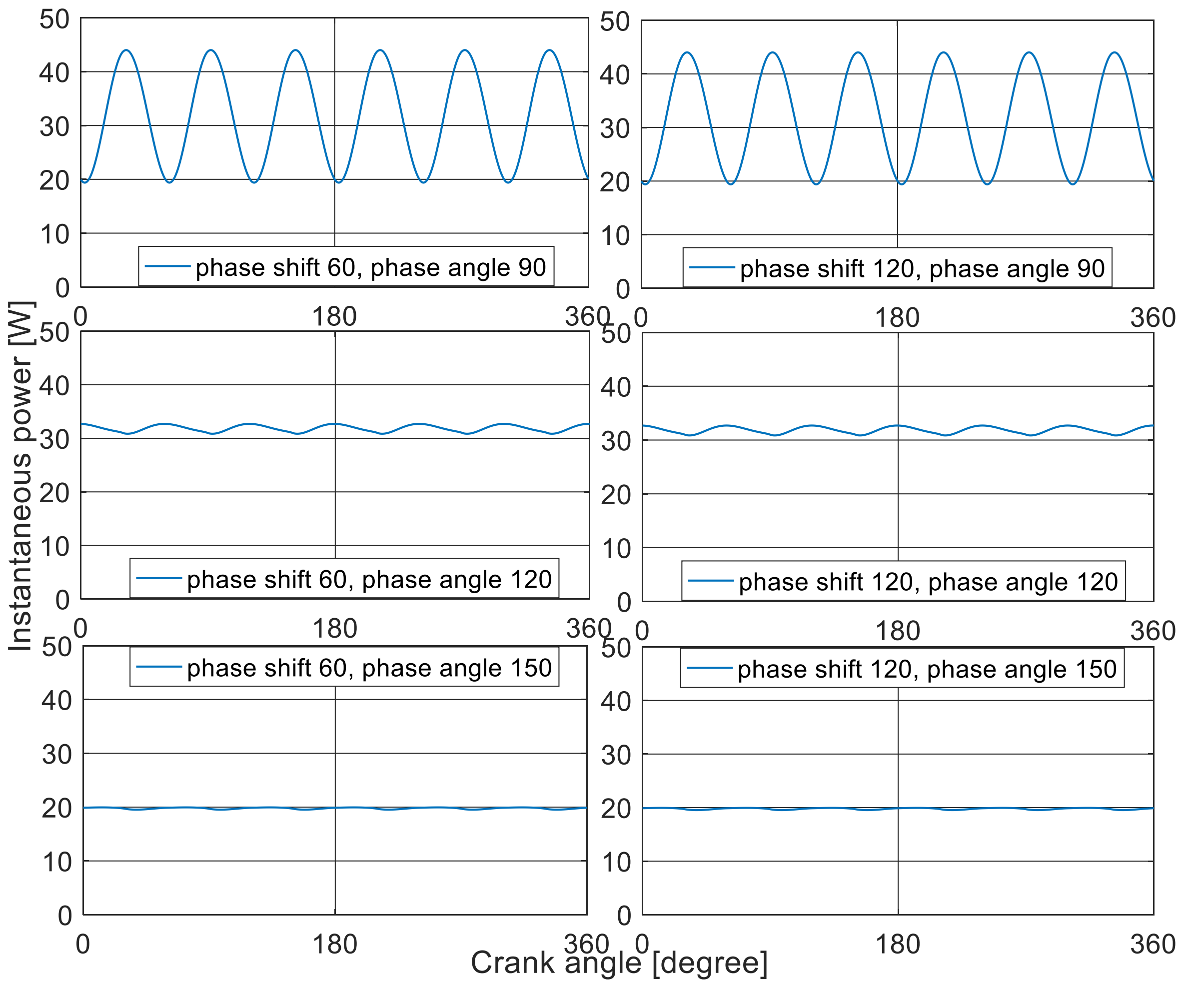

Figure 13: Effect of the phase angle on the power variation of a 3-ph Franchot engine at 60º and 120º phase shifts.

3.4 Multi-phase $(n - ph)$ Franchot engine

The different power signals of a multi-phase engine are added to the crankshaft. As seen in Figure 7, the 1-ph engine has a power frequency, which is two times the engine rotational frequency and thus each phase has two maxima and two minima in one cycle. In order to remove the negative power durations, each negative power duration must be balanced by positive power durations. In the multi-phase engine, the phase shifts can be chosen with the aim of cancelling the maxima and minima.

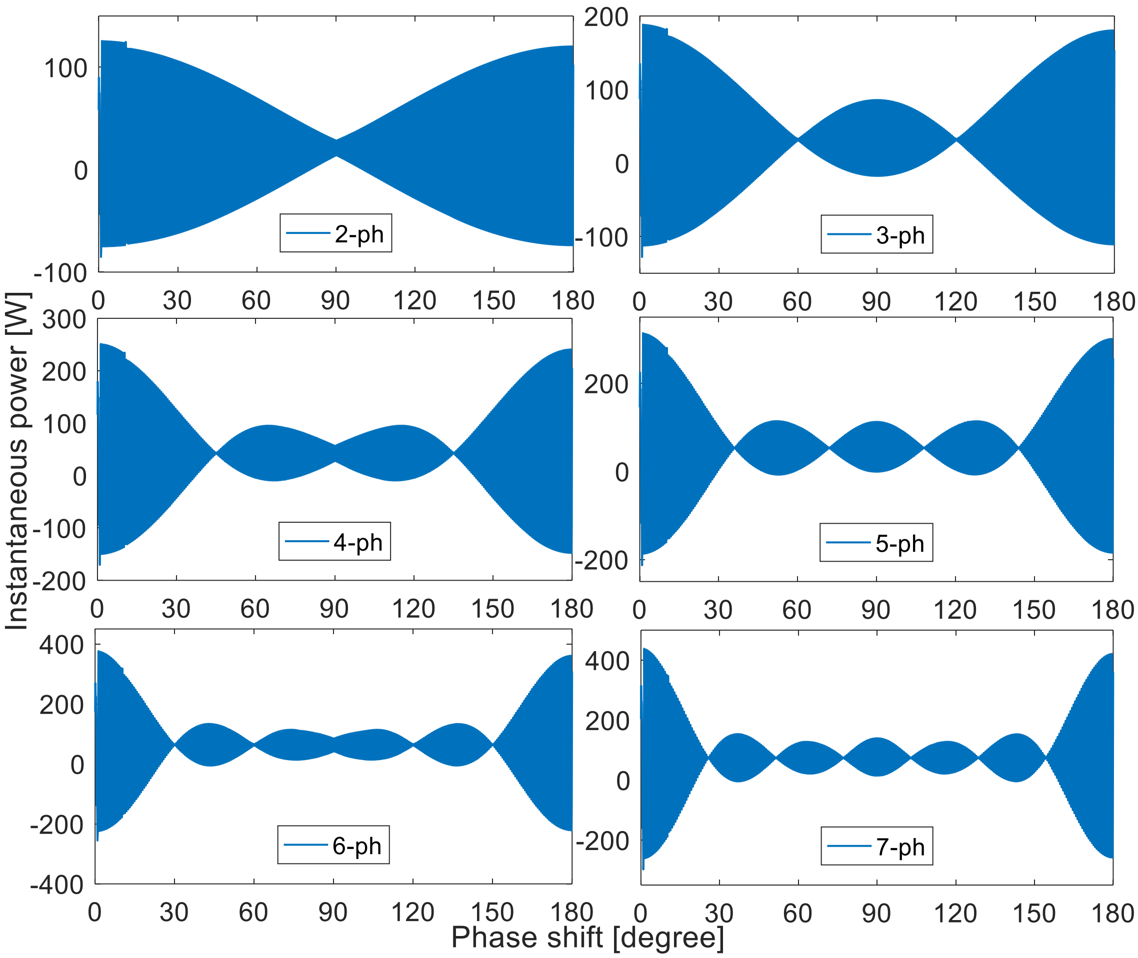

Figure 14: Power amplitude response of the multi-phase Franchot engine with the phase shift.

Figure 14 shows the power amplitude for the 2-ph to 7-ph Franchot engines over the phase shift. For each $n-ph$ engine, there are $n-1$ different phase shifts which produce power variation minima. The phase shifts that lead to the lowest power variations are given by

$$\theta_s = \frac{180}{n} y \qquad 32$$

where y is an integer between 1 and $n-1$, n is the number of phases (pair of hot and cold cylinders) of the Franchot engine. For even y values, the Franchot engines will be uniformly distributed around the crankshaft making a symmetric phase shift between the adjacent engines. The minimum phase shift of the uniformly distributed $n-ph$ Franchot engine is twice the phase shift of an equivalent Siemens configuration and is given by

$$\theta_s = \frac{360}{n} \qquad 33$$

For odd y values, the Franchot engines will be stacked on one half of the crankshaft making the smallest phase shift equal to

$$\theta_s = \frac{180}{n} \qquad 34$$

Those two phase shifts have the same effect on the power signal because each Stirling engine in a Franchot engine completes a power cycle in one rotation and the two power cycle are shifted by 180°. In another word, the power cycle frequency of a Franchot engine is twice that of the Stirling engine which makes each Franchot engine complete a power signal cycle in half a rotation. As the power is non-dimensional and due to the Franchot opposite engines, the instantaneous power at a phase shift of θ is equivalent to the instantaneous power $at\ 180^o - \theta$ and hence, it is mirrored about 90°. At the phase shift of 90°, the angular shift in the power signal is $180n$. Hence, for an even number of phases this results in a signal duplication for which the signal amplitude is amplified instead of being filtered.

Since the phase shift is valid for $y \leq n - 1$, the minimum number of phases that results in power minima and have symmetric distribution is three since y needs to be an even number. Symmetric distribution of phases uniformly distributes the forces and masses on the crankshaft, which reduces the vibrations encountered by them. In order to reduce the vibrations related to the rocking couples, there should be pairs of expansion and compression pistons that move simultaneously in the same direction. Thus, the phase angle must be fixed based on the phase shift. However, for $n > 4$, different phase angles can be obtained due to the regenerator connections. For example, for $n = 5$ the expansion volume $v_{e,k}$ might be connect to the compression volume $v_{c,k+1}$ or $v_{c,k+2}$ which would result in different phase angles.

Table 3 summarises the potential phase angles up to the $8 - ph$ Franchot engine where the phases are uniformly distributed around the crankshaft. These phase angles can be mathematically described by Equation 32, which is also used to calculate the phase shift, but only for even y. These phase angles are similar to the phase angles of the multi-cylinder single-acting Stirling engine [7].

Table 3: Phase angle of the multi cylinder Franchot engine

	3-ph	*4-ph*	*5-ph*	*6-ph*	*7-ph*	*8-ph*
$\boldsymbol{y}$=2	*120°*	*90°*	*72°*	*60°*	*51.4°*	*45°*
$\boldsymbol{y}$=4			*144°*	*120°*	*102.8°*	*90°*
$\boldsymbol{y}$=6					*154.2°*	*135°*

4 Conclusion

The phasor diagram and a reduced multi-cylinder model are used to obtain the power signal to evaluate the vibrations and self-starting capabilities of multi-cylinder Franchot engines. The polytropic model shows good agreement with the performance curves from a published experimental study. It is shown that the multi-cylinder Franchot engines are self-starting if at least two Franchot engines are combined. In addition, the cranks can be evenly distributed for three or more Franchot engines. Finally, the power oscillation can be reduced for the $n - ph$ engine, which agrees with the reported cases. Hence, the slider crank mechanism is recommended for the $n - ph$ Franchot engine where $n \geq 3$ as it is able to reduce the power pulses, rocking couples and primary vibrations caused by each Franchot engine on the rotating crankshaft. On the other hand, the slider crank mechanism does not remove the rocking couples in the Siemens configuration. In addition, the 3-ph Franchot engine gives a preferable phase angle of 120° in contrast to 60° of an equivalent Siemens configuration. Thus, the multi-cylinder Franchot engine can be self-starting, has significantly reduced vibrations and can use the simple slider crank mechanism.

Acknowledgement

The authors would like to thank the British Council - HESPAL for the Ph.D scholarship for Jafar M. Daoud.

References

[1] G. Walker, “Coal-fired Stirling engines for railway locomotive and stationary power applications,” *Proc lnstn Mech Engrs*, vol. 197A, no. October, pp. 233–246, 1983.

[2] B. Hoegel, D. Pons, M. Gschwendtner, and A. Tucker, “Theoretical investigation of the performance of an Alpha Stirling engine for low temperature applications,” *ISEC Int. Stirling Engine Comm.*, no. January, 2012.

[3] M. H. Ahmadi, M.-A. Ahmadi, and F. Pourfayaz, “Thermal models for analysis of performance of Stirling engine: A review,” *Renew. Sustain. Energy Rev.*, vol. 68, no. October 2016, pp. 168–184, 2017.

[4] D. G. Thombare and S. K. Verma, “Technological development in the Stirling cycle engines,” *Renew. Sustain. Energy Rev.*, vol. 12, no. 1, pp. 1–38, Jan. 2008.

[5] G. Fenies, F. Formosa, J. Ramousse, and A. Badel, “Double acting Stirling engine: Modeling, experiments and optimization,” *Appl. Energy*, vol. 159, pp. 350–361, 2015.

[6] G. Walker, *Cryocoolers*, Part 1: Fu. Boston, MA: Springer US, 1983.

[7] S. Chatterton and P. Pennacchi, “Design of a Novel Multicylinder Stirling Engine,” *J. Mech. Des.*, vol. 137, no. 4, p. 042303, 2015.

[8] D. M. Berchowitz and Y.-R. KWon, “Multiple-cylinder, free-piston, alpha configured Stirling engines and heat pumps with stepped pistons,” U.S. Patent 7,171,811 B1, 2007.

[9] J. Arthur A. Varela, “Hybrid electric propulsion system,” U.S. Patent 5,172,784 A, 1992.

[10] A. Høeg, T.-M. Tveit, T. Aase, and T.-A. Asphjell, “Mechanical Design of the 4-500 KWth stirling cycle heat pump SPP 4-106,” in *The 17th International Stirling Engine Conference*, 2016, pp. 21–33.

[11] P. Fette, “A Stirling Engine Able to Work with Compound Fluids Using Heat Energy of Low to Medium Temperatures,” in *Sixth International Stirling Engine Conference*, 1993, pp. 13–18.

[12] T. Finkelstein, “Optimization of phase angle and volume ratio for Stirling engines,” Jan. 1960.

[13] T. Finkelstein and A. J. Organ, *Air Engines*. 2001.

[14] M. A. White, J. E. Augenblick, and A. A. Peterson, “Double acting thermodynamically resonant free-piston multicylinder Stirling system and method,” U.S. Patent 7,134,279 B2, 2006.

[15] B. Hoegel, “Thermodynamics-based design of stirling engines for low-temperature heat sources.,” University of Canterbury, 2014.

[16] H. Damirchi, G. Najafi, S. Alizadehnia, R. Mamat, C. S. Nor Azwadi, W. H. Azmi, and M. M. Noor, “Micro Combined Heat and Power to provide heat and electrical power using biomass and Gamma-type Stirling engine,” *Appl. Therm. Eng.*, vol. 103, pp. 1460–1469, 2016.

[17] C. Çınar, F. Aksoy, H. Solmaz, E. Yılmaz, and A. Uyumaz, “Manufacturing and testing of an A-type Stirling engine,” *Appl. Therm. Eng.*, vol. 130, pp. 1373–1379, 2018.

[18] H. Karabulut, “Dynamic model of a two-cylinder four-stroke internal combustion engine and vibration treatment,” *Int. J. Engine Res.*, vol. 13, no. 6, pp. 616–627, Dec. 2012.

[19] D. Ipci and H. Karabulut, “Thermodynamic and dynamic modeling of a single cylinder four stroke diesel engine,” *Appl. Math. Model.*, vol. 40, no. 5–6, pp. 3925–3937, 2016.

[20] T. K. Garrett, K. Newton, and W. Steeds, “Engine balance,” in *Motor Vehicle*, Elsevier, 2000, pp. 25–46.

[21] J. M. Daoud and D. Friedrich, “Performance investigation of a novel Franchot engine design,” *Int. J. Energy Res.*, Aug. 2017.

[22] J. M. Daoud and D. Friedrich, “Parametric Study of an Air Charged Franchot Engine with Novel Hot and Cold Isothermalizers,” *Inventions*, vol. 2, no. 4, p. 35, Dec. 2017.

[23] J. M. Daoud and D. Friedrich, “A novel Franchot engine design based on the balanced compounding method,” *Energy Convers. Manag.*, vol. 169, pp. 315–325, Aug. 2018.

[24] J. Mou and G. Hong, “Startup mechanism and power distribution of free piston Stirling engine,” *Energy*, vol. 123, pp. 655–663, Mar. 2017.

[25] M. Pfabe and C. Woernle, “Reducing torsional vibrations by means of a kinematically driven flywheel - Theory and experiment,” *Mech. Mach. Theory*, vol. 102, pp. 217–228, 2016.

[26] M. Costea and M. Feidt, “The effect of the overall heat transfer coefficient variation on the optimal distribution of the heat transfer surface conductance or area in a Stirling engine,” *Energy Convers. Manag.*, vol. 39, no. 16–18, pp. 1753–1761, Nov. 1998.

[27] F. Toda, S. Iwamoto, M. Matsuo, and Y. Umezane, “Heat Transfer on a Small Stirling Engine,” *J. Mar. Eng. Soc. JAPAN*, vol. 25, no. 6, pp. 358–365, 1990.

[28] H. Karabulut, H. S. Yucesu, and A. Koca, “Manufacturing and testing of a V-type Stirling engine,” *Turkish J. Eng. Environ. Sci.*, vol. 24, no. 2, pp. 71–80, 2000.

[29] C. H. Cheng and Y. J. Yu, “Numerical model for predicting thermodynamic cycle and thermal efficiency of a beta-type Stirling engine with rhombic-drive mechanism,” *Renew. Energy*, vol. 35, no. 11, pp. 2590–2601, 2010.

[30] B. Kongtragool and S. Wongwises, “Thermodynamic analysis of a Stirling engine including dead volumes of hot space, cold space and regenerator,” *Renew. Energy*, vol. 31, no. 3, pp. 345–359, Mar. 2006.

[31] M. Tanaka, I. Yamashita, and F. Chisaka, “Flow and Heat Transfer Characteristics of the Stirling Engine Regenerator in an Oscillating Flow,” *JSME Int. J.*, vol. 33, no. 2, pp. 283–289, 1990.

[32] M. Babaelahi and H. Sayyaadi, “Simple-II: A new numerical thermal model for predicting thermal performance of Stirling engines,” *Energy*, vol. 69, pp. 873–890, May 2014.